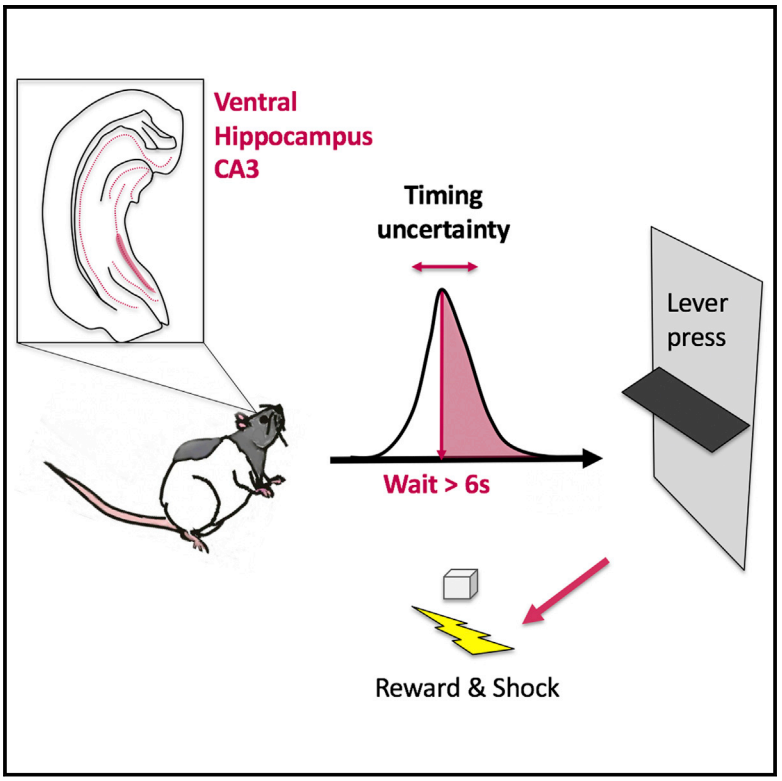
Cell Reports

The ventral hippocampus CA3 is critical in regulating timing uncertainty in temporal decision-making

Graphical Abstract



Authors

Bilgehan Çavdaroğlu, Sadia Riaz, Yuqing Shi, Fuat Balcı, Rutsuko Ito

Correspondence

rutsuko.ito@utoronto.ca

In Brief

The neural substrate of timing uncertainty, an inherent component of optimal temporal decision making, is not well known. Using a temporal decision-making task combined with chemogenetics, Çavdaroğlu et al. demonstrate that pyramidal cells in the CA3 subregion of the ventral hippocampus are important in modulating timing uncertainty.

Highlights

- Rats learn to time their responses for mixed (reward + shock) outcomes
- Rats wait longer to respond for reward + higher shock duration (higher conflict)
- Ventral hippocampus CA3 (vCA3) inhibition reduces timing uncertainty
- vCA3 modulates variability of decision threshold setting and/or switch closure latency

Çavdaroğlu et al., 2021, Cell Reports *34*, 108694
February 2, 2021 © 2021 The Author(s).
https://doi.org/10.1016/j.celrep.2021.108694

Cell Reports

CellPress
OPEN ACCESS

Report

The ventral hippocampus CA3 is critical in regulating timing uncertainty in temporal decision-making

Bilgehan Çavdaroğlu,[1] Sadia Riaz,[1] Yuqing Shi,[1] Fuat Balcı,[2] and Rutsuko Ito[1,3,4,*]
[1]Department of Psychology, University of Toronto Scarborough, Toronto, ON, Canada
[2]Department of Psychology and Center for Translational Medicine, Koç University, Istanbul, Turkey
[3]Department of Cell and Systems Biology, University of Toronto, Toronto, ON, Canada
[4]Lead contact
*Correspondence: rutsuko.ito@utoronto.ca
https://doi.org/10.1016/j.celrep.2021.108694

SUMMARY

Timing uncertainty is a critical component of temporal decision-making, as it determines the decision strategies that maximize reward rate. However, little is known about the biological substrates of timing uncertainty. In this study, we report that the CA3 subregion of the ventral hippocampus (vCA3), a relatively unexplored area in timing, is critical in regulating timing uncertainty that informs temporal decision making. Using a variant of the differential reinforcement of low rates of responding (DRL) task that incorporates differential levels of approach-avoidance conflict, rats were trained to wait a minimum of 6 s to earn a reward that was paired with varying durations of foot shock. Post-training chemogenetic inhibition of the vCA3 reduced timing uncertainty without affecting mean wait times, irrespective of the level of conflict experienced. Simulations based on the information-processing variant of scalar expectancy theory (SET) revealed that the vCA3 may be important in modulating decision threshold or switch closure latency variability.

INTRODUCTION

The ability to time is a ubiquitous component of our cognition observed across many species (Boisvert and Sherry, 2006; Staddon, 1965). The prevalence of timing mechanisms is unsurprising since adaptive behaviors entail the consideration of temporal regularities and relationships in the environment, in order to optimize reward rates (e.g., during foraging; (Brunner et al., 1992)). Although the study of the optimality of temporal decisions is a burgeoning field, temporal decisions that are made under conflict (e.g., when punishment accompanies reward) and the underlying neural circuitry are seldom studied, despite their adaptive significance (e.g., timing of foraging with the threat of predation).

Timed responses exhibit substantial variability between individual trials as a manifestation of endogenous timing uncertainty. This inherent variability affects timing performance in many timing tasks such as the differential reinforcement of low rates of responding (DRL) (e.g., Ferster and Skinner, 1957; Çavdaroğlu et al., 2014), and it is typically assumed to be resistant to improvement. In the DRL task, animals are trained to wait for a minimum amount of time (schedule) between responses to obtain a reward. Although responding right after the minimum wait time would seem to be the optimal strategy, this strategy results in forfeiting virtually half of the available rewards due to the inevitable timing uncertainty. In fact, constrained temporal precision requires agents to aim for waiting longer than the minimum wait time to reduce the risk of resultant response not meeting the schedule criterion, albeit at the expense of increased time cost of rewards.

In addition to endogenous timing uncertainty, exogenous variables such as probabilistic relationships and reward magnitude also adaptively guide temporal decisions (e.g., Akdoğan and Balcı, 2016; Balci et al., 2009). Increasing the reward magnitude or reward sensitivity shifts the onset of timing behavior (Balci et al., 2013; Ludvig et al., 2007, 2011) or time of maximal reward expectancy (Galtress and Kirkpatrick, 2009) leftward in the peak interval (PI) procedure and results in shorter wait times in DRL tasks (Doughty and Richards, 2002). Despite these known interactions between reward magnitude and timing, it is not clear whether coupling the reward with punishment would shift the wait times rightward as would be predicted if they have an additive effect.

While traditionally associated with learning and memory processes (Eichenbaum, 2000; Squire and Wixted, 2011), the hippocampus (HC) is richly implicated in arbitrating reward-punishment conflict (Fried and Goddard, 1967; Kimble, 1963; Kimura, 1958; Niki, 1962) and learned approach-avoidance conflict (Ito and Lee, 2016). Furthermore, HC damage results in timing deficits, inducing a leftward shift in timed responses in PI (Meck et al., 1987; Olton et al., 1988) and DRL (Deacon et al., 2005; Johnson et al., 1977; Schmaltz and Isaacson, 1966) tasks. Conflict processing is thought to be preferentially mediated by the ventral HC (VH, Schumacher et al., 2016, 2018; Ito and Lee,

This is an open access article under the CC BY-NC-ND license (http://creativecommons.org/licenses/by-nc-nd/4.0/).

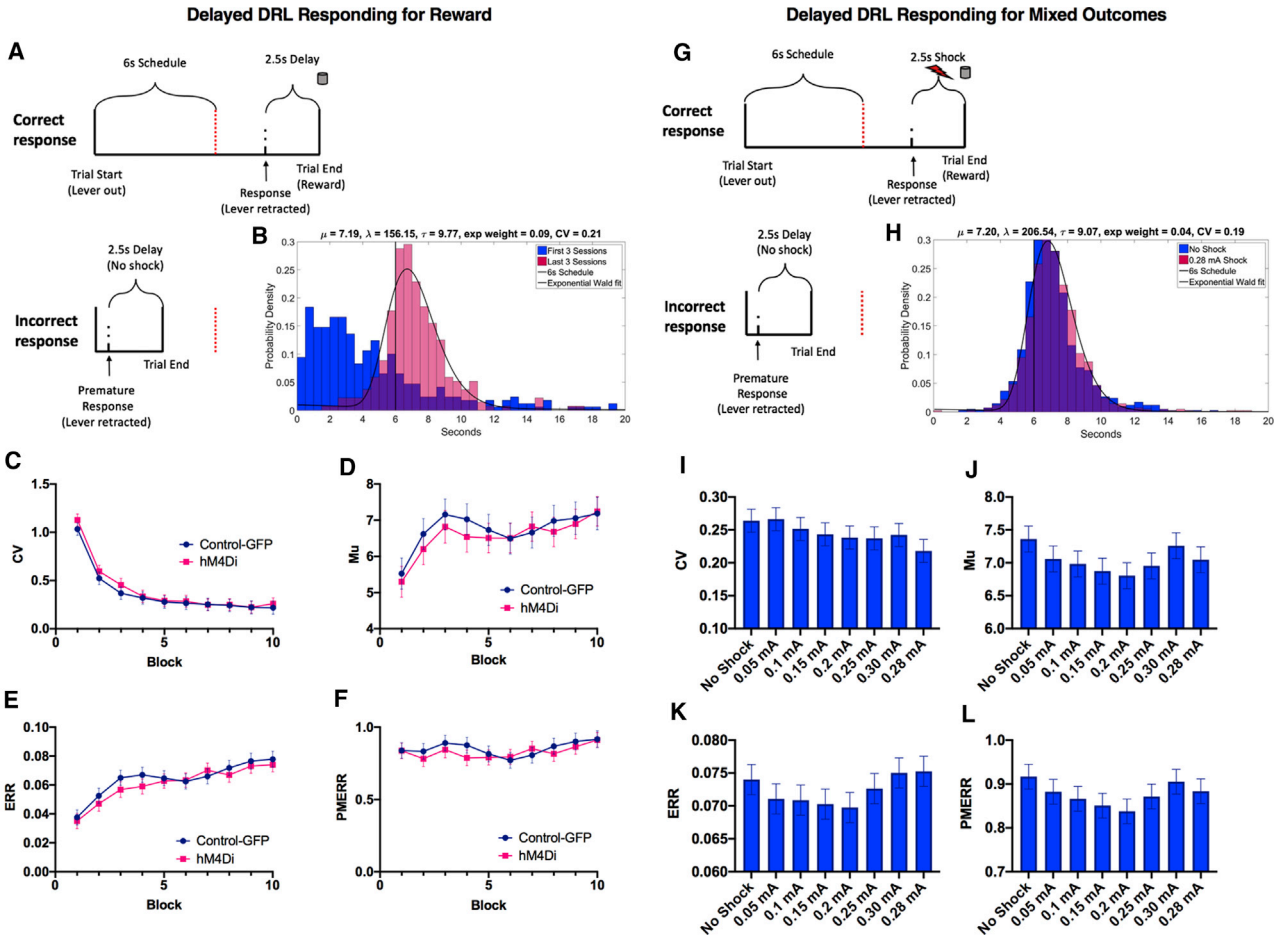


Figure 1. Delayed DRL responding for reward, and mixed outcomes

(A) Schematic representation of delayed DRL task. All responses made after the schedule (6 s) were rewarded with a sucrose pellet 2.5 s after the lever press. Premature responses shorter than the schedule were not rewarded.

(B) Normalized inter-response time densities for the first and last three sessions of training (out of a total of 30 sessions).

(C–F) Future virus surgery groups (hM4Di versus GFP) performed similarly in timing uncertainty (CV) (C), average wait time (mu) (D), expected reward rate (ERR) (E), and percentage of maximum expected reward rate (PMERR) (F).

(G) Schematic representation of mixed outcomes DRL task. All responses made after the schedule (6 s) were rewarded with a sucrose pellet and 2.5-s foot shock (starting at 0.05 mA). The shock intensity was increased every six sessions by 0.05 mA until 0.3 mA was reached. Premature responses made before the schedule were not rewarded.

(H) Normalized inter-response time densities for no shock and 0.28 mA shock conditions.

(I–L) Increasing the shock intensity induced a significant decrease in timing uncertainty (CV) (I), and U-shaped changes in the wait duration (mu) (J), ERR (K), and PMERR (L). All data shown as mean values ± SEM.

2016), whereas temporal processing has been more readily associated with the dorsal HC (DH) (Tam et al., 2013, 2015; Yin and Meck, 2014; but see Bannerman et al., 1999, Oprisan et al., 2018). However, the role of the VH in timing behavior has been underexplored (Lee et al., 2020), and very little is known about the underlying biological substrates of timing variability.

The goals of the present study were twofold: (1) to test whether having a mixed outcome of shock and reward pellet in the DRL task has an effect similar to changing the reward value, and (2) to investigate the differential effects of chemogenetic VH inhibition on timing behavior and its optimality with and without conflicting outcomes. We hypothesized that the addition of shock to the reward outcome will delay wait times, mimicking the effect of reduction in reward value, while chemogenetic inhibition of VH will alter DRL performance only in temporal decisions made under conflict conditions.

RESULTS

Animals successfully acquired the delayed DRL schedule of responding for reward

Animals were first trained to acquire a delayed (2.5-s) DRL (6-s DRL) for a reward pellet (Figures 1A and 1B) in which they were required to wait a minimum of 6 s before responding for a reward. Analysis of the acquisition data across 10 blocks of three sessions revealed that timing uncertainty decreased (coefficient of

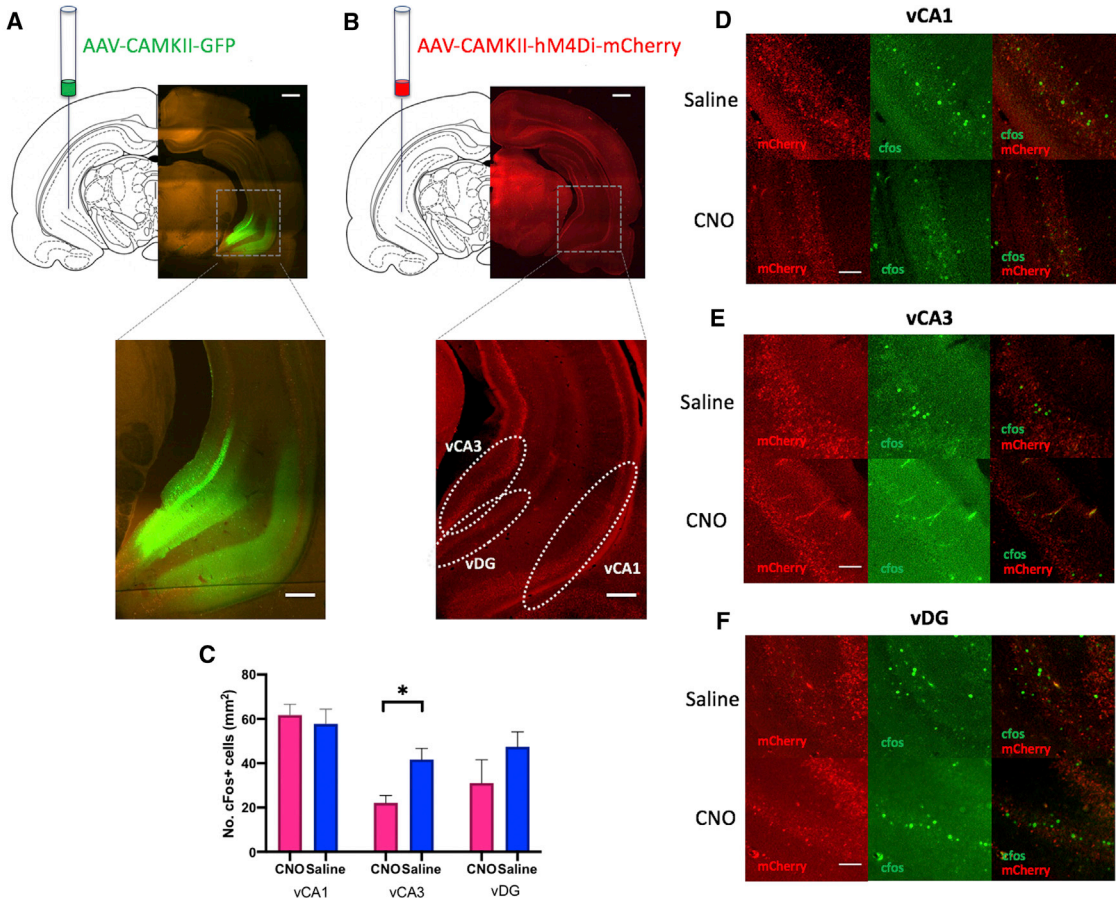


Figure 2. Immunohistochemical validation of hM4Di-mediated VH inhibition

(A and B) Targeted locations and expression of the control GFP and hM4Di in the VH. Scale bars: top images, 1 mm; inset images, 500 μm.

(C) The number of cfos$^+$ cells (per mm^2) in hM4Di-expressing rats that had received saline or clozapine-*N*-oxide (CNO) were counted in ×4 images in three regions of interest: ventral CA1 (vCA1), ventral CA3 (vCA3), and ventral dentate gyrus (vDG). There was a significant reduction in the cfos$^+$ cell count in the vCA3 region only. *$p < 0.05$.

(D–F) Representative ×10 images showing mCherry/hM4Di expression, cfos expression, and co-localization of hM4Di-mCherry$^+$ and cfos$^+$ cells in the vCA1 (D), vCA3 (E), and vDG (F) of saline- versus CNO-administered rats. Scale bars: 100 μm. All data are shown as mean values ± SEM.

variation [CV], $F(9, 182.72) = 160.22$, $p < 0.0001$, Figure 1C), and wait time ($F(9, 182.59) = 11.85$, $p < 0.0001$, Figure 1D), expected reward rate (ERR, $F(9, 182.58) = 50.77$, $p < 0.0001$, Figure 1E), and percentage of maximum expected reward rate (PMERR, $F(9, 182.33) = 4.80$, $p < 0.001$, Figure 1F) increased as training progressed. Thus, training improved task performance and, as expected, an increase in EER (i.e., more rewards per unit time) accompanied the improvement in temporal precision. There was no interaction between block number and future virus group assignment in terms of the CV ($F(9, 182.72) = 0.77$, $p = 0.64$), wait time (mu, $F(9, 182.59) = 0.55$, $p = 0.83$), ERR ($F(9, 182.58) = 1.32$, $p = 0.23$), or PMERR ($F(9, 182.33) = 1.23$, $p = 0.28$) during training. Thus, there was no difference in the speed or pattern of task acquisition between the construct groups before the surgery.

CNO induced reduction in cfos$^+$ cells in the vCA3, but not vCA1 or vDG

Animals then underwent surgery to inject the inhibitory hM4Di construct or control GFP into the VH using an AAV vector. Immunohistochemical analysis revealed that all animals, except one, showed robust expression of hM4Di (mCherry$^+$ cells) or GFP within the confines of the VH (Figure 2). Furthermore, in order to verify that the administration of clozapine-*N*-oxide (CNO) induced the desired inhibition of the VH, we assessed the number of cfos$^+$ pyramidal cells in VH subregions of animals expressing hM4Di receptors. Analysis of the number of cfos$^+$ cells activated after an additional high-conflict test session revealed that the group that was injected with CNO had reduced cfos active cells in the CA3 region of VH ($t(5) = 3.03$, $p = 0.03$) but not in CA1 ($t(5) = 0.45$, $p = 0.67$) or in DG (dentate gyrus, $t(5) = 1.38$, $p = 0.23$) compared to those injected with saline, providing evidence for regional specificity of the inhibition (Figure 2C).

Animals successfully acquired the delayed DRL schedule of responding for mixed outcomes

After surgery, rats continued their DRL training, now with mixed outcomes (of increasing levels of a 2.5-s foot shock plus reward) in order to establish the point of reward-punishment conflict that

the rats could tolerate (Figures 1G and 1H). Incrementally increasing the shock intensity by 0.05 mA every six sessions did not interfere with overall responding until 0.30 mA, at which point three animals stopped responding. We therefore established a 2.5-s 0.28 mA shock to be the highest point of reward-punishment conflict.

Incremental increases in shock intensity led to a gradual and persistent reduction in the CV ($F(7, 315) = 8.10$, $p < 0.0001$, Figure 1I), but U-shaped changes in wait time ($F(7, 315) = 8.17$, $p < 0.0001$, Figure 1J), ERR ($F(7, 315) = 6.79$, $p < 0.0001$, Figure 1K), and PMERR ($F(7, 315) = 8.04$, $p < 0.0001$, Figure 1L) with a minima at 0.2 mA shock intensity. There was no significant difference between performance measures in the no shock and 0.28 mA shock (last) conditions in terms of wait times ($t(22) = 1.10$, $p = 0.14$), ERR ($t(22) = 1.90$, $p = 0.07$) or PMERR ($t(22) = 0.47$, $p = 0.68$), but a significant reduction in the CV ($t(22) = 3.33$, $p = 0.003$). These alterations in timing performance may therefore have been caused by animals adjusting to shock delivery after their surgery and/or by the extra training session animals received. Importantly, future group assignment did not interact with the effect of shock intensity on the CV ($F(7, 315) = 1.12$, $p = 0.35$), wait time ($F(7, 315) = 0.65$, $p = 0.71$), ERR ($F(7, 315) = 0.56$, $p = 0.79$), or PMERR ($F(7, 315) = 0.30$, $p = 0.96$).

In summary, the introduction of escalating shock did not induce notable changes in the response patterns beyond a decrease in the CV and transient perturbations of wait times, ERR and PMERR, which stabilized at 0.28 mA.

Higher shock duration lengthens wait times and increases the CV, but inhibition of the VH decreases the CV

Next, animals were tested in the mixed outcome DRL task in which the degree of reward-punishment conflict was changed every six sessions by varying the duration of shocks (0, no conflict; 1.5 s, medium conflict; and 2.5 s, high conflict; Figure 3A), starting with the highest conflict sessions first (i.e., at the shock level they were trained with), and ending with the no-conflict sessions. In the first three sessions of each conflict condition, animals in both the hM4Di and control-GFP groups received saline injections prior to the test session to establish/re-establish baseline performance. In the latter three sessions, all animals received CNO (1 mg/kg) injections prior to testing. A linear mixed model including the three shock durations, drug (CNO or saline), and the construct group (hM4Di designer receptors exclusively activated by designer drugs [DREADDs] or control-GFP) was used to analyze response patterns in mixed outcome DRL tests. We found that the CV was significantly higher in sessions with the highest shock duration ($F(2, 110) = 10.51$, $p < 0.0001$, Figures 3B and 3F) and also uncovered a significant interaction between drug and the construct group ($F(1, 110) = 6.83$, $p = 0.01$). This interaction was driven by the CNO injection in the hM4Di group causing a significant overall decrease in the CV compared to saline injections, irrespective of shock duration ($p = 0.004$). No other comparisons were significant (e.g., GFP saline versus GFP-CNO, $p = 0.48$; hM4Di-saline versus GFP-saline, $p = 0.23$; hM4Di-CNO versus GFP-CNO, $p = 0.92$).

Furthermore, there was a significant main effect of shock duration on wait times ($F(2, 115) = 48.0$, $p < 0.0001$, Figures 3C and 3G), irrespective of drug (CNO/saline, drug: $F(1, 110) = 1.17$, $p = 0.28$). Animals waited longer at the highest shock duration in both the hM4Di and GFP groups. Consistently, increases in shock duration also increased both the ERR ($F(2, 184.94) = 17.48$, $p < 0.0001$, Figure 3D and 3H) and PMERR ($F(2, 110) = 35.81$, $p < 0.0001$, Figures 3E and 3I). The control GFP group exhibited higher indices of optimality in general, regardless of drug (CNO or saline): ERR ($F(1, 21) = 8.02$, $p < 0.01$) and PMERR ($F(1, 21) = 4.51$, $p < 0.05$), compared to the hM4Di group. The cause of this closer-to-optimal performance in the GFP group is unclear, but it could speak to the large individual differences we observed in DRL performance with mixed outcomes, which necessitated the implementation of a within-subject design in our study. Thus, the most meaningful data are derived from our within-subject comparisons.

In summary, higher shock durations increased the CV and wait times, which were accompanied by increases in ERR and PMERR (i.e., closer to optimal responding). Importantly, CNO injections reduced the CV in the hM4Di group under all conflict conditions, when compared to their performance after saline injections, without affecting the other three parameters.

VH inhibition effect on the CV can be explained by reduced threshold setting variability and/or switch closure latency variability

The information-processing variant of scalar expectancy theory (SET) is a prominent model of interval timing (e.g., Gibbon et al., 1984). According to SET, a hypothetical pacemaker emits clock pulses that start to be accumulated in working memory (WM) when an ''attentional switch" closes with the start of the to-be-timed event. With the delivery of reinforcement at the end of the time interval, the accumulation of pulses stops due to the termination of the gating of pulses with the (re-)opening of the same switch mechanism. The resultant WM representation of elapsed time is consolidated into long-term memory (LTM), during which it is assumed to be subject to perturbation of normally distributed random noise. Subsequently, the current time stored in WM is continually compared to the expected time of reinforcement randomly sampled from LTM, and when the values reach a certain threshold (which itself can be a random variable, Gibbon and Church, 1990), the timed response is emitted. Although the psychophysical properties of interval timing can be accounted for in a number of different ways, including the pacemaker variability across trials and temporal integration rates that are inversely proportional to the target durations (e.g., Treisman, 1963; Simen et al., 2013), SET conventionally assumes that it is the perturbation that occurs during the transfer of temporal information to LTM and the ratio-based decision rule that give rise to the scalar property (namely the constancy of the CV for different target intervals; Gibbon et al., 1984).

Within this theoretical framework, we postulated that the observed CNO-induced reduction in CV in the *absence of an effect on the mean wait times* in the hM4Di group can be explained most parsimoniously by the modulation of two variables, that is, the level of trial-to-trial variability in the decision threshold

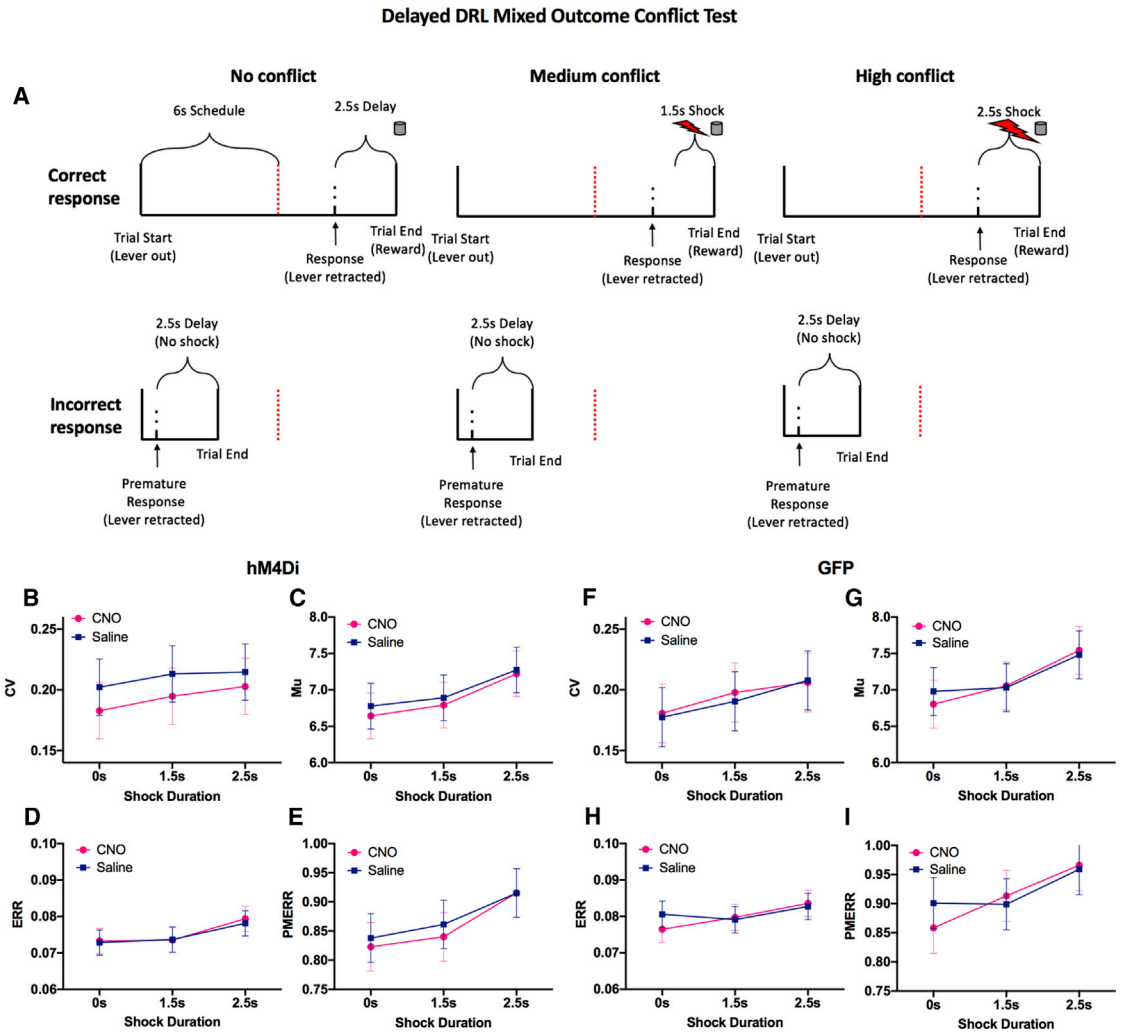


Figure 3. DRL mixed outcome conflict test

(A) Schematic representation of DRL responding under mixed outcome conflict. All responses made after the schedule (6 s) were reinforced with a sucrose pellet 2.5 s after the lever press for the no shock condition, while animals received 1.5- and 2.5-s shocks (0.28 mA) that co-terminated with a sucrose pellet delivery in the medium-conflict and high-conflict conditions, respectively. Premature responses emitted before the schedule were not reinforced.

(B–I) Both hM4Di (B–E) and control-GFP groups (F–I) were tested in each conflict condition for six sessions, including three sessions with saline injections, followed by three sessions with systemic CNO injections (1 mg/kg) in a within-subjects design. There was a significant reduction in timing uncertainty (CV) (B) for the hM4Di group only with CNO injection while there was no difference in the GFP group (F). There was no significant effect of CNO injection in either group for wait time (mu) (C and G), ERR (D and H), or PMERR (E and I). All data are shown as mean values ± SEM.

setting or switch closure latency. If we assume that VH inhibition results in a reduced standard deviation of threshold setting and/or latency of switch closure (upon the onset of time event) without affecting their average values, this would lead to a narrower distribution of response times (i.e., reduced CV) without altering the mean response time. In order to demonstrate these relationships, we conducted numerical simulations within the framework of SET with three different values for threshold setting variability (SD of 0.3, 0.2, and 0.1) and switch closure latency variability (SD of 1.5, 1 and 0.5). Visual inspection of the results in Figure 4 showed that the central tendency of the wait times remains stable while their variability decreases with both reduced threshold setting and switch closure latency variability.

DISCUSSION

The present study was motivated by the fact that the role of VH in timing processes has remained relatively unexplored. To this end, we investigated the effect of chemogenetically inhibiting the pyramidal neurons in the CA3 subregion of VH on steady-state DRL responding for reward, as well as a variant of DRL, in which rats performed DRL responding under an approach-avoidance conflict. We report two important findings. First, intensifying the degree of approach-avoidance conflict by increasing the shock duration increased the wait time and decreased timing precision. Second, counter to our prediction, inhibition of the CA3 subregion

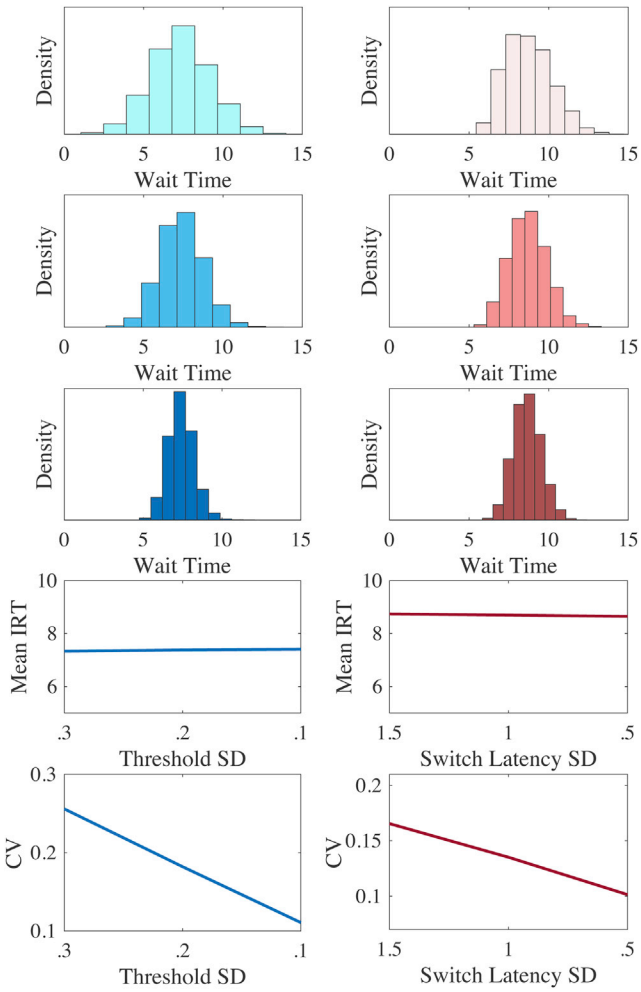


Figure 4. Simulation results for threshold and switch closure latency variability

The top left three panels show the distributions of the threshold first crossing times for threshold setting SD of 0.3, 0.2, and 0.1, respectively, while the top right three panels show the first crossing times for the switch closure latency SD of 1.5, 1, and 0.5. The fourth and fifth panels show that the mean wait time is not affected by these manipulations, but the CV of wait times decreases robustly with decreasing variability of these parameters.

of the VH *improved* timing precision in rats, independent of the level of conflict experienced. In contrast to previous DH lesion studies that reported a leftward shift in wait times and impaired timing precision (Deacon et al., 2005; Johnson et al., 1977; Schmaltz and Isaacson, 1966, Tam et al., 2015), we did not find an effect of VH CA3 inhibition on wait times. Furthermore, there was no effect of VH inhibition on ERR or PMERR, even though both measures were sensitive to shock duration, ruling out the potential role of VH in the optimization of temporal decisions. Taken together, we have identified the glutamatergic neurons in the CA3 subregion of the VH to be critical in regulating timing uncertainty/variability.

Rats can learn and perform DRL responses for reward accompanied by low-intensity shock

Punishment of responses emitted prior to the DRL schedule has been a feature in DRL tasks for pigeons (Holz et al., 1963), monkeys (Galbicka and Branch, 1981), rats (Bruner. 1967), and even humans (Çavdaroğlu et al., 2014). However, responding under the DRL schedule for mixed outcomes has not been well investigated in rats. Consistent with earlier work (Freestone et al., 2015), our rats took around 30 sessions to master DRL responding. The transition from DRL responding for reward only to mixed outcomes was seamless; however, DRL performance for reward accompanied by increasing shock intensities was initially more variable, with transient changes in wait times, ERR, and PMERR, which subsequently stabilized at the highest shock level. The shape of the wait time distributions was invariant under different outcome conditions. However, we did observe a decrease in CV as training progressed with increasing shock intensities, which could be attributed to a reduction in timing uncertainty based on the animals learning new task rules (Freestone et al., 2015), in addition to changes in shock value. Thus, after sufficient training animals learn to tolerate the administration of shock in order to obtain reward, and our results suggest that the mixed outcome DRL schedule can be used reliably in rats to study approach-avoidance conflict.

Wait times, CV, expected reward rate, and optimality are sensitive to the presence of approach-avoidance conflict

Our results demonstrated that DRL responding under high approach-avoidance conflict was accompanied by longer wait times. One possible explanation for this effect is that there was a decrease in impulsive responding that corresponds to the non-timed exponential component of the response distribution (Holz et al., 1963), but this possibility is not empirically supported since there was an absence of a prominent exponential component in the DRL mixed outcome conditions. Instead, the observed rightward shift in wait times is similar to what is seen in the PI procedure when animals receive lithium chloride, which induces gastric malaise (Galtress and Kirkpatrick, 2009). Thus, the longer wait times are likely caused by the effect of the approach-avoidance conflict on one or more components of the timing mechanism (decision and/or clock stage). However, the observed increase in CV with longer shock durations suggests at least an additional (timing strategy-independent) effect of the conflict level on DRL responding. In other words, the conflict manipulation appears to also introduce variance in DRL responding from sources other than the scalar timing mechanism (e.g., conflict monitoring, response inhibition). Further studies are warranted to dissect the contributions of temporal and non-temporal factors to the observed effects.

Inhibition of vCA3 reduces the CV for all conflict conditions

Surprisingly, inhibition of glutamatergic pyramidal neurons in the vCA3 reduced the CV across all approach-avoidance conflict conditions (including no conflict), indicating that this effect was timing related, rather than being specific to the presence of an approach-avoidance conflict. This observation is remarkably reminiscent of a previous finding using the PI procedure, in which

VH lesions, but not DH or sham lesions, led to a reduction in response variability in a 45-s PI schedule, in addition to an increase in stop times, when response rates were normalized (Yin and Meck, 2014). While the timing procedures used and the biological manipulations used to quantify timing uncertainty were different, the findings of Yin and Meck, along with the present data, implicate a role for VH in mediating the uncertainty characteristics of timing. Note that this VH role in timing contrasts with the proposed role of the DH in timing precision and accuracy (Tam et al., 2013, 2015). Excitotoxic lesions of the DH have been shown to *increase* the CV and response variability in PI timing (Tam et al., 2015), raising the intriguing possibility that the DH and VH subserve opposing roles in regulating timing uncertainty.

More specifically, the reductions in CV in the absence of a change in wait times, together with our numerical simulations, suggest that vCA3 modulates the trial-to-trial variability of timing decision threshold and/or the closure switch latency. Of these two possibilities, altered switch closure latency variability in particular can be prone to disruption by the carryover effects of the shock experience in the previous trial on the subsequent attentional gating of temporal information. For instance, a weaker (e.g., working memory) trace of a recent aversive experience as a result of vCA3 inhibition might result in the "contribution" of lower noise into the onset of temporal gating function (assuming that such traces prospectively modulate attention) in the next trial due to lower trial-to-trial fluctuations in the strength of memory traces. Indeed, this possibility is highly consistent with previous reports of VH, or more specifically vCA3, inactivation attenuating the expression of passive avoidance of both a shock-associated context and cues that elicit approach-avoidance conflict (Ambrogi Lorenzini et al., 1997; Schumacher et al., 2018). Furthermore, a weakened trial-based feedback control of memory sampling has previously been shown in rats with fimbria fornix lesions, where they were less likely to incorporate information from previous trials to guide the determination of their temporal criterion in the current trial, further substantiating hippocampal involvement in trial-to-trial variability of interval timing (Meck, 1988). A similar rationale can also be applied to the reduced threshold variability over longer timescales as a result of carry-over effects. That being said, this possibility is not fully supported by our empirical results since the timing uncertainty gains were also observed in the no-shock condition. Still, it is possible that the disruption in VH-based memory trace is linked to the experience of reward delivery rather than, or in addition to, the shock experience. However, here again, our findings reveal that VH inhibition did not have a differential effect on the CV of responses emitted after a trial that yielded outcomes, as opposed to responses that were made after a trial that was not reinforced (Figure S1). Thus, the CNO-induced effects are likely manifested mechanistically rather than being mediated by the resultant effects on auxiliary factors (such as memory trace).

Another possible explanation is that vCA3-inhibited animals in the present study may have been applying a stricter criterion when comparing the remembered schedule time with the actual duration timed in the current trial, with memory samples shorter than the schedule not becoming re-integrated into LTM. The dorsal CA3, with its recurrent collateral networks, has been commonly linked to pattern completion of spatial and object memory, which is the ability to recall a whole memory based on partial or incomplete cues (Knierim and Neunuebel, 2016; Marr, 1971; McNaughton and Morris, 1987; McNaughton and Nadel, 1990; Myers and Scharfman, 2009; Rolls and Kesner, 2006; Treves and Rolls, 1994; Yassa and Stark, 2011; Kesner et al., 2016). While speculative, the present data may implicate the vCA3 in the process of generalization/pattern completion (applying a liberal criterion in the reintegration of memory samples that are further away from the wait schedule committed to LTM) in the realm of temporal memory. In a study by Kesner et al. (2016), dorsal CA3 lesions induced a deficit in object pattern completion, with the degree of performance deficit increasing with a reduction in the number of object cues available (degradation of recall cues: 4 to 1), indicating increased sensitivity to larger mismatches between the original memory and recall conditions. Similarly, in our experiment, the timing schedule is already represented in LTM from previous training. According to our SET-based simulation, in each DRL trial, a response is generated based on a random sample from LTM (which determines the target time) after it is scaled with a normally distributed random threshold value (which along with the sample from LTM determines the response time) (Gibbon et al., 1984). The CA3 inhibition-induced reduction in the variability of the threshold parameter might simply result from the same dynamics that underlie increased sensitivity to a memory-recall mismatch.

Finally, the absence of an effect of vCA3 inhibition on temporal decision-making under approach-avoidance conflict was unexpected given previous findings implicating the vCA3 and vCA1 in regulating cued approach-avoidance conflict (Schumacher et al., 2018). That being said, accumulating evidence suggests that the VH may be particularly important in regulating goal-directed behaviors under the control of cues that signal potential reward or threat, as opposed to actual appetitive/aversive outcomes, with the present task falling into the latter category. Thus, approach-avoidance conflict situations that are sensitive to VH lesions, such as the elevated plus maze, the cued approach-avoidance conflict maze, or even cued extinction sessions, are all instances in which stimulus features signal safety/reward or threat in the absence of actual outcomes (Bannerman et al., 2004; Schumacher et al., 2016, 2018; Çavdaroğlu et al., 2020, 2021). However, this possibility clearly warrants further investigation.

In conclusion, using a variant of DRL responding in which animals are required to make timing decisions under approach-avoidance conflict, we have found that timing uncertainty and wait times are modulated by shock duration. We also identified the vCA3 as a critical neural substrate of timing uncertainty, which contrasts with the previously observed role of the DH in timing precision. Simulations based on SET revealed the vCA3 to be particularly important in modulating decision threshold variability or switch closure latency variability. Given the known role of the CA3 (albeit more for dorsal CA3) in spatial and object pattern completion processes, it is conceivable that the vCA3 plays a role in comparing the temporal proximity of the experienced duration with the generated sample from reference memory.

STAR★METHODS

Detailed methods are provided in the online version of this paper and include the following:

- KEY RESOURCES TABLE
- RESOURCES AVAILABILITY
  - Lead contact
  - Materials availability
  - Data and code availability
- EXPERIMENTAL MODEL AND SUBJECT DETAILS
- METHOD DETAILS
  - Surgery
  - Drug injections
  - Behavioral procedures
  - cfos Immunohistochemistry
  - Cell imaging and counting
- QUANTIFICATION AND STATISTICAL ANALYSIS
  - Simulation Details

SUPPLEMENTAL INFORMATION

Supplemental Information can be found online at https://doi.org/10.1016/j.celrep.2021.108694.

ACKNOWLEDGMENTS

This study was funded by the Natural Sciences and Engineering Research Council of Canada (NSERC) of Canada awarded to R.I. (402642). We are grateful to Dr. Maithe Arruda Carvalho for providing the training and use of a Nikon fluorescent microscope.

AUTHOR CONTRIBUTIONS

Conceptualization, B.C. and R.I.; methodology, B.C. and R.I.; investigation, B.C., Y.S., and S.R.; formal analysis, B.C. and F.B.; visualization, B.C., F.B., and R.I.; writing – original draft, B.C., F.B., and R.I.; writing – review & editing, B.C., F.B., and R.I.; funding acquisition, R.I.; supervision, R.I.

DECLARATION OF INTERESTS

The authors declare no competing interests.

Received: May 13, 2020
Revised: November 30, 2020
Accepted: January 4, 2021
Published: February 2, 2021

REFERENCES

Akdoğan, B., and Balcı, F. (2016). Stimulus probability effects on temporal bisection performance of mice (*Mus musculus*). Anim. Cogn. *19*, 15–30.

Ambrogi Lorenzini, C.G., Baldi, E., Bucherelli, C., Sacchetti, B., and Tassoni, G. (1997). Role of ventral hippocampus in acquisition, consolidation and retrieval of rat's passive avoidance response memory trace. Brain Res. *768*, 242–248.

Balci, F., Freestone, D., and Gallistel, C.R. (2009). Risk assessment in man and mouse. Proc. Natl. Acad. Sci. USA *106*, 2459–2463.

Balcı, F., Wiener, M., daroğlu, B., and Branch Coslett, H. (2013). Epistasis effects of dopamine genes on interval timing and reward magnitude in humans. Neuropsychologia *51*, 293–308.

Bannerman, D.M., Yee, B.K., Good, M.A., Heupel, M.J., Iversen, S.D., and Rawlins, J.N.P. (1999). Double dissociation of function within the hippocampus: a comparison of dorsal, ventral, and complete hippocampal cytotoxic lesions. Behav. Neurosci. *113*, 1170–1188.

Bannerman, D.M., Rawlins, J.N.P., McHugh, S.B., Deacon, R.M., Yee, B.K., Bast, T., Zhang, W.N., Pothuizen, H.H.Z., and Feldon, J. (2004). Regional dissociations within the hippocampus—memory and anxiety. Neurosci. Biobehav. Rev. *28*, 273–283.

Bates, D., Mächler, M., Bolker, B., and Walker, S. (2015). Fitting linear mixed-effects models using lme4. J. Stat. Softw. *67*, 1–48.

Boisvert, M.J., and Sherry, D.F. (2006). Interval timing by an invertebrate, the bumble bee *Bombus impatiens*. Curr. Biol. *16*, 1636–1640.

Bruner, A. (1967). Food-based timing behavior sharpened by the selective punishment of short interresponse times. Psychon. Sci. *8*, 187–188.

Çavdaroğlu, B., Zeki, M., and Balci, F. (2014). Time-based reward maximization. Philos. Trans. R. Soc. Lond. B Biol. Sci. *369*, 20120461.

Brunner, D., Kacelnik, A., and Gibbon, J. (1992). Optimal foraging and timing processes in the starling, Sturnus vulgaris: effect of inter-capture interval. Anim. Behav. *44*, 597–613.

Çavdaroğlu, B., Riaz, S., Yeung, E.H.L., Lee, A.C.H., and Ito, R. (2021). The ventral hippocampus is necessary for cue-elicited, but not outcome driven approach-avoidance conflict decisions: a novel operant choice decision-making task. Neuropsychopharmacology *46*, 632–642.

Çavdaroğlu, B., Toy, J., Schumacher, A., Carvalho, G., Patel, M., and Ito, R. (2020). Ventral hippocampus inactivation enhances the extinction of active avoidance responses in the presence of safety signals but leaves discrete trial operant active avoidance performance intact. Hippocampus *30*, 913–925.

Deacon, R.M.J., Reisel, D., Perry, V.H., Nicholas, J., and Rawlins, P. (2005). Hippocampal scrapie infection impairs operant DRL performance in mice. Behav. Brain Res. *157*, 99–105.

Doughty, A.H., and Richards, J.B. (2002). Effects of reinforcer magnitude on responding under differential-reinforcement-of-low-rate schedules of rats and pigeons. J. Exp. Anal. Behav. *78*, 17–30.

Eichenbaum, H. (2000). A cortical-hippocampal system for declarative memory. Nat. Rev. Neurosci. *1*, 41–50.

Ferster, C.B., and Skinner, B.F. (1957). Differential reinforcement of rate. Schedules of Reinforcement (Appleton-Century-Crofts), pp. 464–507.

Flaherty, C.F. (1996). Problems in the Behavioural Sciences, No. 15: Incentive Relativity (Cambridge University Press).

Freestone, D.M., Balcı, F., Simen, P., and Church, R.M. (2015). Optimal response rates in humans and rats. J. Exp. Psychol. Anim. Learn. Cogn. *41*, 39–51.

Fried, P., and Goddard, G. (1967). The effects of hippocampal lesions at different stages of conflict in the rat. Physiol. Behav. *2*, 325–330.

Galbicka, G., and Branch, M.N. (1981). Selective punishment of interresponse times. J. Exp. Anal. Behav. *35*, 311–322.

Galtress, T., and Kirkpatrick, K. (2009). Reward value effects on timing in the peak procedure. Learn. Motiv. *40*, 109–131.

Gibbon, J., and Church, R.M. (1990). Representation of time. Cognition *37*, 23–54.

Gibbon, J., Church, R.M., and Meck, W.H. (1984). Scalar timing in memory. Ann. N Y Acad. Sci. *423*, 52–77.

Holz, W.C., Azrin, N.H., and Ulrich, R.E. (1963). Punishment of temporally spaced responding. J. Exp. Anal. Behav. *6*, 115–122.

Ito, R., and Lee, A.C.H. (2016). The role of the hippocampus in approach-avoidance conflict decision-making: evidence from rodent and human studies. Behav. Brain Res. *313*, 345–357.

Johnson, C.T., Olton, D.S., Gage, F.H., 3rd, and Jenko, P.G. (1977). Damage to hippocampus and hippocampal connections: effects on DRL and spontaneous alternation. J. Comp. Physiol. Psychol. *91*, 508–522.

Kesner, R.P., Kirk, R.A., Yu, Z., Polansky, C., and Musso, N.D. (2016). Dentate gyrus supports slope recognition memory, shades of grey-context pattern separation and recognition memory, and CA3 supports pattern completion for object memory. Neurobiol. Learn. Mem. *129*, 29–37.

Kimble, D.P. (1963). The effects of bilateral hippocampal lesions in rats. J. Comp. Physiol. Psychol. *56*, 273–283.

Kimura, D. (1958). Effects of selective hippocampal damage on avoidance behavior in the rat. Canad. J. Psychol. Rev./Canad. Psychol. *12*, 213–218.

Knierim, J.J., and Neunuebel, J.P. (2016). Tracking the flow of hippocampal computation: pattern separation, pattern completion, and attractor dynamics. Neurobiol. Learn. Mem. *129*, 38–49.

Lee, A.C.H., Thavabalasingam, S., Alushaj, D., Çavdaroğlu, B., and Ito, R. (2020). The hippocampus contributes to temporal duration memory in the context of event sequences: a cross-species perspective. Neuropsychologia *137*, 107300.

Ludvig, E.A., Conover, K., and Shizgal, P. (2007). The effects of reinforcer magnitude on timing in rats. J. Exp. Anal. Behav. *87*, 201–218.

Ludvig, E.A., Balci, F., and Spetch, M.L. (2011). Reward magnitude and timing in pigeons. Behav. Processes *86*, 359–363.

Marr, D. (1971). Simple memory: a theory for archicortex. Philos. Trans. R. Soc. Lond. B Biol. Sci. *262*, 23–81.

McNaughton, B.L., and Morris, R.G.M. (1987). Hippocampal synaptic enhancement and information storage within a distributed memory system. Trends Neurosci. *10*, 408–415.

McNaughton, B.L., and Nadel, L. (1990). Hebb-Marr networks and the neurobiological representation of action in space. In Neuroscience and Connectionist Theory, M.A. Gluck, ed. (Lawrence Earlbaum Associates), pp. 1–63.

Meck, W.H. (1988). Hippocampal function is required for feedback control of an internal clock's criterion. Behav. Neurosci. *102*, 54–60.

Meck, W.H., Church, R.M., Wenk, G.L., and Olton, D.S. (1987). Nucleus basalis magnocellularis and medial septal area lesions differentially impair temporal memory. J. Neurosci. *7*, 3505–3511.

Myers, C.E., and Scharfman, H.E. (2009). A role for hilar cells in pattern separation in the dentate gyrus: a computational approach. Hippocampus *19*, 321–337.

Niki, H. (1962). [Effects of hippocampal ablation upon conditioned behavior in the rat]. Sogo Igaku *19*, 524–528.

Olton, D.S., Wenk, G.L., Church, R.M., and Meck, W.H. (1988). Attention and the frontal cortex as examined by simultaneous temporal processing. Neuropsychologia *26*, 307–318.

Oprisan, S.A., Buhusi, M., and Buhusi, C.V. (2018). A population-based model of the temporal memory in the hippocampus. Front. Neurosci. *12*, 521.

Pellegrini, S., López Seal, M.F., and Papini, M.R. (2008). Scaling relative incentive value: different adjustments to incentive downshift in pigeons and rats. Behav. Processes *79*, 182–188.

Rolls, E.T., and Kesner, R.P. (2006). A computational theory of hippocampal function, and empirical tests of the theory. Prog. Neurobiol. *79*, 1–48.

Schmaltz, L.W., and Isaacson, R.L. (1966). Retention of a DRL 20 schedule by hippocampectomized and partially neodecorticate rats. J. Comp. Physiol. Psychol. *62*, 128–132.

Schumacher, A., Vlassov, E., and Ito, R. (2016). The ventral hippocampus, but not the dorsal hippocampus is critical for learned approach-avoidance decision making. Hippocampus *26*, 530–542.

Schumacher, A., Villaruel, F.R., Ussling, A., Riaz, S., Lee, A.C.H., and Ito, R. (2018). Ventral hippocampal CA1 and CA3 differentially mediate learned approach-avoidance conflict processing. Curr. Biol. *28*, 1318–1324.e4.

Simen, P., Rivest, F., Ludvig, E.A., Balci, F., and Killeen, P. (2013). Timescale invariance in the pacemaker-accumulator family of timing models. Timing Time Percept. *1*, 159–188.

Squire, L.R., and Wixted, J.T. (2011). The cognitive neuroscience of human memory since H.M. Annu. Rev. Neurosci. *34*, 259–288.

Staddon, J.E.R. (1965). Some properties of spaced responding in pigeons. J. Exp. Anal. Behav. *8*, 19–27.

Tam, S.K., Jennings, D.J., and Bonardi, C. (2013). Dorsal hippocampal involvement in conditioned-response timing and maintenance of temporal information in the absence of the CS. Exp. Brain Res. *227*, 547–559.

Tam, S.K., Jennings, D.J., and Bonardi, C. (2015). Effects of dorsal hippocampal damage on conditioning and conditioned-response timing: a pooled analysis. Hippocampus *25*, 444–459.

Treisman, M. (1963). Temporal discrimination and the indifference interval. Implications for a model of the "internal clock". Psychol. Monogr. *77*, 1–31.

Treves, A., and Rolls, E.T. (1994). Computational analysis of the role of the hippocampus in memory. Hippocampus *4*, 374–391.

Yassa, M.A., and Stark, C.E.L. (2011). Pattern separation in the hippocampus. Trends Neurosci. *34*, 515–525.

Yin, B., and Meck, W.H. (2014). Comparison of interval timing behaviour in mice following dorsal or ventral hippocampal lesions with mice having δ-opioid receptor gene deletion. Philos. Trans. R. Soc. Lond. B Biol. Sci. *369*, 20120466.

STAR★METHODS

KEY RESOURCES TABLE

REAGENT or RESOURCE	SOURCE	IDENTIFIER
Antibodies		
Anti-c-Fos antibody	Synaptic Systems	Cat# 226 003; RRID:AB_2231974
Peroxidase AffiniPure F(ab')$_2$ Fragment Donkey Anti-Rabbit IgG (H+L)	Jackson Immunoresearch	Cat#711-036-152; RRID:AB_2340590
Bacterial and virus strains		
pAAV-CaMKIIa-hM4D(Gi)-mCherry	Addgene	Cat# 50477-AAV8, RRID:Addgene_50477
pAAV-CaMKIIa-EGFP	Addgene	Cat#50469-AAV8,RRID:Addgene_50469
Chemicals, peptides, and recombinant proteins		
Clozapine-N-Oxide	Tocris	Cat # 6329
Deposited Data		
Behavioral data for Figures 1, 3, and 4		https://doi.org/10.17632/pcbp6k6n4h.1
Experimental models: organisms/strains		
Long Evans rats	Charles River	Cat#2308852;RRID:RGD_2308852
Software and algorithms		
Med-PC IV	Med Associates	https://www.med-associates.com/
Graphpad Prism 8	Graphpad	https://www.graphpad.com

RESOURCES AVAILABILITY

Lead contact

Further information and requests for resources and reagents should be directed to and will be fulfilled by the Lead Contact, Rutsuko Ito (rutsuko.ito@utoronto.ca).

Materials availability

This study did not generate new unique reagents.

Data and code availability

The datasets supporting the current study have been deposited on Mendeley Data: https://doi.org/10.17632/pcbp6k6n4h.1.

EXPERIMENTAL MODEL AND SUBJECT DETAILS

Subjects were 23 male Long Evans rats (Charles River, QC, Canada), weighing ~400-600 g at the time of surgery. They were housed in groups of two per cage in a 21°C room, under a 12hr light/dark cycle (lights on at 7:00 A.M.). Water was available *ad libitum* throughout the experiment. Before commencing behavioral testing, food was restricted to maintain animals' weights around 90% of their free feeding weight to promote motivation to engage in behavioral tasks. All behavioral testing took place in accordance with the ethical and legal requirements under Ontario's Animals for Research Act, the federal Canadian Council on Animal Care, and approval of the Local Animal Care Committee.

METHOD DETAILS

Surgery

Rats were divided into two groups (n = 12 hM4Di-injected treatment group; n = 11 GFP-injected controls) and underwent bilateral adeno-associated virus (AAV) injection surgeries. Rats in the treatment group were anaesthetized with isoflurane gaseous anesthetic (4%–5% for induction, 2%–3% for maintenance, Benson Medical, ON, Canada) and placed in a stereotaxic frame (Stoelting Co, IL). Briefly, an incision was made at the skull midline and small holes were created via a dental drill to target the VH bilaterally (AP −5.6mm; ML ± 5.0mm; DV −6.5mm). A 10 μL Hamilton syringe was then lowered into the VH for bilateral infusion of 0.5 μL

of AAV containing inhibitory Designer Receptors Exclusively Activated by Designer Drugs (DREADDs) hM4Di (AAV8-CAMKII-hM4Di-mCherry) and CAMKII promoter to drive selective expression of the receptors and red fluorescent protein mCherry in the pyramidal (glutamatergic) cells of target VH. The AAV delivery occurred over a period of 5min with a controlled electronic microinjector (Stoelting Co, IL). Once injection was completed, the syringe remained at the delivery site for an additional 5min to allow AAV particles to diffuse away from the injector tip before the scalp was sutured back together. The same surgical procedure was implemented in the control rats, but a control virus (AAV8-CAMKII-GFP) was delivered instead of DREADD-hM4Di. This virus lacked the inhibitory receptors, but contained a CAMKII promoter to drive the expression of green fluorescent protein tag GFP, in glutamatergic cells of the target VH for visualization of the transduction. After surgery, the animals were allowed a recovery period of a minimum of 7 days with post-surgical care and food available *ad libitum* before further behavioral testing.

Drug injections

All rats received an intraperitoneal (IP) injection of either 0.9% saline or clozapine-N-oxide (CNO, dissolved in 2.5% DMSO and diluted in sterile saline at a volume of 1ml/kg), a selective pharmacological actuator of hM4Di receptors, to selectively inhibit VH glutamatergic neurons expressing the receptors, 45min prior to each testing session for the delayed DRL mixed outcome conflict tests (see later for detailed description).

Behavioral procedures

Apparatus

Testing took place in 8 operant chambers (30.5 cm L × 24.1 cm W × 29.2 cm H, Med Associates, VT) contained within a sound-attenuated box with a ventilation fan. Primary components of each chamber included two 4cm wide retractable levers positioned on the sidewall, located 2cm from either side of a central food well (magazine) and 5cm above the floor composed of parallel shock bars. A light panel was positioned 3cm above each lever. The shock bars were connected to scrambled shock generators (ENV-414, Med Associates, VT), which produced mild foot shocks (up to 2.5 s in duration and 0.30mA in intensity) to cause the subjects brief peripheral discomfort, but not freezing. A pellet dispenser attached to the central food well delivered 45mg chocolate sucrose pellets (TestDiet, MO) as reward stimuli, and an infrared detector monitored every nose poke entry into the food well. The chamber was illuminated by a 1.8W, 17V house light located at the top right corner of the chamber.

Pre-training

All rats received two magazine training sessions in which they were placed in the operant box for one hour and received sucrose pellets on a variable interval 20 s schedule of reinforcement.

Following magazine training, the rats were trained to lever press for sucrose pellets under a Fixed Ratio 1 schedule. The side of the lever to be inserted was randomly chosen until 50 rewards were obtained from each side to avoid side bias. A session ended after 30 minutes, or after animals pressed both levers 50 times. Rats were moved to the next phase of training after two consecutive sessions with at least 40 presses on each side.

Delayed differential reinforcement of low rates of responding (DRL) schedule

Following lever press training, all rats were tested in the Delayed DRL schedule of reinforcement. Trials started with the insertion of either the left or right lever and rats were required to wait a fixed minimum time duration (6 s) before responding to obtain a sucrose pellet. If the subject responded prematurely, then the lever was retracted without reward and the trial ended 2.5 s after the retraction. When a correct response was executed, the lever retracted immediately, and the delivery of the reward pellet came at a delay of 2.5 s following the lever retraction. The next trial started immediately after the end of the previous trial, and each session was terminated after 50min. The 2.5 s delayed DRL schedule was implemented in order to accommodate the introduction of shocks in the next phase of training. After 30 sessions, training was halted for the rats to undergo surgical infusions of the hM4Di/control construct.

Delayed DRL mixed outcome training

After recovery from surgery, all rats were trained under the same DRL schedule, but now with the addition of a mild foot shock (2.5 s, 0.05mA to begin with) along with the reward delivery 2.5 s after the lever press response. Shock intensity was increased incrementally by 0.05 mA every 6 sessions until it reached 0.30mA, in order to establish the 'break point' at which animals stopped responding. For the remainder of the sessions, shock intensity was reduced to and fixed at 0.28mA to promote responding under 'tolerable' levels of conflict. Animals were administered a total of 50 sessions in this phase of training.

Delayed DRL mixed outcome conflict test

All rats underwent three sets of 6 DRL mixed outcome conflict test sessions at three different conflict levels, which was implemented by pairing 1 reward pellet with decreasing durations of the 0.28mA shock: high conflict (2.5 s 0.28mA shock with 1 pellet), medium conflict (1.5 s 0.28mA shock with 1 pellet), and no conflict (no shock with 1 pellet) and presented in that order for all subjects. This order was chosen to minimize the unpredictable effects of incentive relativity, in which large shifts in reward or shock value can cause distortion in responding (Flaherty 1996; Pellegrini et al., 2008). Manipulations of shock duration, as opposed to shock intensity, was also chosen as the method of modulating conflict levels due to the fluctuations in timing responses and parameters generated by increasing the shock intensity during the training period. For each set of 6 sessions, all subjects were injected with saline prior to the initial three sessions, followed by CNO administration prior to the latter three sessions, such that baseline responding could be re-established after each change in shock duration, and so that *within-subject comparisons* of DRL performance measures with and without CNO could be made at each conflict level.

cfos Immunohistochemistry

All rats were anaesthetized with a lethal dose of pentobarbital and perfused intracardially at the ascending aorta with 0.9% saline, then a 4% paraformaldehyde solution 90 minutes following the end of an additional test session under high conflict, prior to which half of the animals in the hM4Di group was injected with saline, and another half with CNO. Brains were harvested and kept in 4% paraformaldehyde and 20% sucrose solution for 24 hours. The brains were then cut into 50 μm thick coronal sections using a vibratome (Leica VT1200S). All sections were treated with 1% hydrogen peroxide, then incubated in 10% normal goat serum (NGS) blocking solution for 2 hr at room temperature and incubated overnight at 4°C with rabbit c-*fos* antibody (1:5000 dilution, Synaptic Systems, Goettingen, Germany). Following incubation with the primary antibody, sections were washed in PBS (3 × 5 min) and incubated overnight with secondary antibody (peroxidase conjugated donkey-anti-rabbit 1:500, Jackson Immunoresearch, Baltimore, PA, USA). The Tyramide Signal Amplification procedure was then employed, using NHS-fluorescein as a dye substrate. After a final round of PBC washes, brain slices were and mounted on gelatin-coated slides and air-dried before being coverslipped with Fluoroshield Mounting medium with DAPI for nuclear staining (Abcam, Cambridge).

Cell imaging and counting

hM4Di and GFP expression, and c-Fos immunoreactivity were subsequently visualized at 4x, 10x and 20x magnification using the NIKON Ni-U upright fluorescent microscope (NIKON, NY, USA). GFP expressing cells and c-Fos positive cells conjugated with TSA-fluorescein were visualized using the FITC filter (excitation: 467 - 498nm; emission: 513 – 556 nm), while hM4Di expressing cells and c-Fos positive cells conjugated with TSA-Rhodamine were visualized using the TexRed filter (excitation: 532 – 587 nm; emission: 608 – 683 nm). Quantification of c-*fos* positive cells was achieved using three images of coronal sections of the VH taken at 4x magnification from each animal. VH subregions were demarcated into CA1, CA3 and DG as regions of interest, and the number of $cfos^{+}$ cells within those boundaries were counted by converting the images into 8-bit and using ImageJ software (Rasband, W.S., U. S. National Institutes of Health, USA), and quantified in a standardized unit of mm2.

QUANTIFICATION AND STATISTICAL ANALYSIS

Average wait times before responding for every three delayed DRL sessions were pooled to obtain representative probability distributions. Pooled data were fitted with exponential inverse-Gaussian mixture distribution based on maximum likelihood estimation using a custom MATLAB script (Çavdaroğlu et al., 2014) and parameters of the fits were used to calculate wait times, timing uncertainty (coefficient of variation, CV, calculated as Standard Deviation/mean) and optimality indices (ERR, PMERR). These optimality measures and distribution parameters were then analyzed using statistical software R (R Core Team, 2020) and *lme4* (Bates et al., 2015).

Evaluation of the DRL data indicated high variability and individual differences in CV values. Thus, linear mixed modeling (LMM) was employed to analyze the DRL performance data from the acquisition, introduction of shock and CNO/Saline injection sessions. Furthermore, sessions under the same conditions (drug, shock duration) were pooled to obtain more representative response distributions. Visual inspection of the data revealed that responding in the first ~50 trials at the start of each session was much lower than the rest of the session for most of the subjects in CNO/Saline injection sessions. These trials (around 17% of data points) were therefore removed from the distribution. Additionally, trials with wait times that were longer than 5 times the schedule were removed (> 30 s, around 1% of data points). This left around 740 trials for generating response distributions for each conflict condition, which is significantly more than the desired > 150 trials for accurate representations of response patterns. An exponential mixture inverse-Gaussian probability density function was fit to the response data to calculate 4 independent timing parameters: 1) wait time (mu), 2) coefficient of variation (CV), 3) expected reward rate (ERR) and 4) percentage of maximum expected reward rate (PMERR). CV was calculated by dividing the standard deviation ($\sqrt{}$ ($mean^3$ /lambda)) by the mean. ERR was calculated by dividing the probability of obtaining a reward (area under the inverse-Gaussian distribution function that falls to the right of the schedule) by the wait time plus 2.5 s (to account for the delay after the lever press). Lastly, PMERR was calculated by dividing the ERR by the maximum expected reward rate that was possible for the subject's CV value. Each of these parameters was subjected to Linear Mixed Effects analysis. ERR and PMERR provided measures of optimality, with greater values indicating higher optimality. For CNO/Saline injection sessions, we entered the duration of the shock (0, 1.5 or 2.5 s), drug (saline or CNO), and construct (hM4Di or control virus) as fixed effects with all their interactions into the model. As random effects, we used intercepts for subjects. Visual inspection of residual plots did not reveal any obvious deviations from homoscedasticity or normality. P values were obtained by likelihood ratio tests of the full model with the effect in question against the model without the effect in question. *Post hoc* analysis was conducted by using emmeans package with Tukey familywise correction. Degrees of freedom were calculated using the Satterthwaite method. Finally, we conducted simulations to model the effects of modulating threshold and switch closure latency variability on the observed alteration in CV with vCA3 inhibition.

Simulation Details

In the simulations, we used a target latency of 6 (arbitrary unit). We implemented a Poisson clock with a mean inter-clock interval of 0.01. Thus, on average, 100 clock signals coded for the time interval of 1 ($^1/_6$ of the target interval in the simulations). The clock signals were integrated into the working memory without a loss (perfect integrator). In each trial, a random sample was picked from the vector of the long-term memory target interval representations (initialized with the target value of 6 at the first trial). The random LTM sample

was multiplied by a normally distributed random variable with a mean of 1.2 to determine the threshold in that trial. This operation introduced an adaptive threshold bias for timed responding in the DRL task (i.e., leading to on average longer than target response time and thus increasing the probability of the timed response being reinforced). We marked the real-time working memory representation of elapsed time that first crosses the adaptive threshold in that trial. If the resultant behavior was indeed longer than the minimum wait time (thus resulting in reinforcement), the memory sample used to determine responding in that trial was re-integrated into the long-term memory. This process was subjected to a normally distributed random variable (typically referred to as the memory translation constant - Gibbon et al., 1984). The long-term memory representation instead of the manifested response time was re-integrated in long-term memory because the behavioral manifestation of timed responding was partially dependent on the adaptive bias in threshold setting that guided the response without changing the representation. Note that the length of the vector used to implement the long-term memory representation increased with each trial.

We ran two sets of simulations. In the first set of simulations, three different SD levels were used to perturb the threshold between different trials (SD = 0.3, 0.2, and 0.1). For each threshold variability level, we ran 10000 trials (a total of 30000 trials). In this first set of simulations, the translation constant was set to 0.03 (note that the same pattern of results holds for higher values of translation constant) and the switch closure latency was set 0. In the second set of simulations, three different values for switch closure latency variability were used (SD: 1.5, 1, and 0.5). The mean switch closure latency was 1.5, the mean threshold setting was 1.2 and threshold variability was set to 0). In this second set of simulations, any switch closure latency shorter than zero was replaced by zero. For each level of switch closure latency variability, we ran 10000 trials (a total of 30000 trials). All simulations started with the highest variability level separately for threshold and switch latency variability.